Internal flow characteristics in scaled pressure-swirl atomizer

Milan Malý[1,*], *Marcel* Sapík [1], *Jan* Jedelský[1], *Lada* Janáčková[1], *Miroslav* Jícha[1], *Jaroslav* Sláma[2] and *Graham* Wigley[3]

[1]Brno University of Technology, Faculty of Mechanical Engineering, Czech Republic
[2]Provyko s.r.o. Czech Republic
[3]Loughborough University, United Kingdom

Abstract. Pressure-swirl atomizers are used in a wide range of industrial applications, e.g.: combustion, cooling, painting, food processing etc. Their spray characteristics are closely linked to the internal flow which predetermines the parameters of the liquid sheet formed at the discharge orifice. To achieve a better understanding of the spray formation process, the internal flow was characterised using Laser Doppler Anemometry (LDA) and high-speed imaging in a transparent model made of cast PMMA (Poly(methyl methacrylate)). The design of the transparent atomizer was derived from a pressure-swirl atomizer as used in a small gas turbine. Due to the small dimensions, it was manufactured in a scale of 10:1. It has modular concept and consists of three parts which were ground, polished and bolted together. The original kerosene-type jet A-1 fuel had to be replaced due to the necessity of a refractive index match. The new working liquid should also be colourless, non-aggressive to the PMMA and have the appropriate viscosity to achieve the same Reynolds number as in the original atomizer. Several liquids were chosen and tested to satisfy these requirements. P-Cymene was chosen as the suitable working liquid. The internal flow characteristics were consequently examined by LDA and high-speed camera using p-Cymene and Kerosene-type jet A-1 in comparative manner.

1 Introduction

Pressure-swirl (PS) atomizers are easy to manufacture and provide good atomization. They are frequently used in various applications where a large surface area of droplets is needed or a surface must be coated by a liquid e.g. combustion, fire suspension or air conditioning. In principle, the pumped liquid is injected via tangential ports into a swirl chamber where it gains a swirl motion, under which it leaves the exit orifice as a conical liquid sheet which consequently breaks up into small droplets due to aerodynamic forces. The centrifugal motion of the swirling liquid creates a low-pressure zone in the centre of the swirl chamber and generates an air core along the centreline. The flow pattern inside the atomizer is rather complex; it is two-phase flow with secondary flow effects. There is a strong link between the internal flow conditions and the resulting spray characteristics; however, not all aspects of the internal flow are well understood.

A number of authors have studied and visualized the internal flow and air core characteristics using transparent models of the PS atomizers. One of the first were Horvay and Leuckel [1, 2] who used scaled transparent modular atomizers with various internal geometries. They investigated different sized inlet ports and geometries of the swirl chamber. They used a mixture of castor (ricinus) oil, tetraline (1,2,3,4- Tetrahydronaphthalene) and turpentine oil as working liquid to match the refraction index. De Keukelare [3] also used scaled PMMA model to measure the flow rate, pressure distribution and the velocity profiles inside the swirl chamber together with the air core dimensions. He used water and presented a correlation of experimental data with theoretical predictions. Chinn and Yule [4] followed, using LDA and high-speed imaging with water as the working liquid to acquire a velocity field inside the atomizers. They used three different swirl chamber geometries (conical, curved and square). Their experimental data of velocity fields and air-core growth are in accordance with CFD predictions.

Due to the complicated geometry of the swirl chamber with its curved surfaces, it is advisable to have the same refractive index for the liquid and atomizer body in order to make optical measurements.

In addition to Horvay and Leuckel [1, 2], Liu [5] and Thomson [6] also used the same liquid mixture (castor oil, tetraline and turpentine oil) which, however, causes chemical degradation of the PMMA parts. Hassan and Dominguez-Ontiveros [7] investigated matching the PMMA refractive index with p-Cymene and a sodium iodide mixture. Due to difficulty of preparation of sodium iodide, its high cost and occurrence of small particles, they preferred p-Cymene. Muguercia [8] matched the refractive index of the glass tube with a mixture of water and sugar and also with a mixture of water and glycerine.

In this paper, the scaled transparent model of a small pressure-swirl atomizer was manufactured from PMAA in which high-speed imaging and LDA measurement were performed. Several liquids with similar refractive indices were tested and discussed in terms of corrosiveness to PMAA. The air-core shape and velocity profiles were measured for two different liquids and the necessity of refractive index matching is discussed.

* Corresponding author: milan.maly@vutbr.cz

2 Experimental setup

The experiments were performed on a specially designed test bench at the Spray laboratory in the Brno University of Technology. All tests were performed at room temperature (25 °C).

The pressurized liquid was supplied by a fuel supply system – see fig. 1. The liquid was pumped by centrifugal pump (3) from the main tank (1) via a filter (2) to the Coriolis mass flow meter (4). Temperature (5) and pressure sensors (7) were mounted before the atomizer (8). The mass flow rate was set by changing pump speed. The spray freely falls into a collector and returns into the main tank.

2.1 The atomizer

The small-sized simplex atomizer as used in a combustion chamber of turbojet aircraft engine, was investigated. Its main dimension are listed in fig. 2. Due to the small dimensions, the optical measurements inside the transparent model would be extremely difficult. For this reason, a scaled transparent copy, with a modular construction was manufactured. It consisted of three pieces, one with the swirl chamber, the second part with the tangential inlet ports and the last one a cap. This construction allowed changing each piece for another with a different geometry thus providing easy modification of the atomizer geometry.

A thin transparent gasket material was used to prevent leakage of the liquid between the interfaces. The inner surfaces of every piece were grounded and polished to achieve transparency for the optical measurements.

2.2 Flow match and tested liquids

The scaled model is ten times larger than the original atomizer and its construction is shown in fig. 3. To maintain the flow behaviour, dimensionless numbers such as Reynolds number, swirl number and Froude number must remain the same as in the original atomizer. Thus a new inlet condition had to be proposed to fulfil these requirements.

The Reynolds number is defined as the ratio of inertial force to the viscous force and it is a crucial parameter that must be maintained to simulate the behaviour of liquid in the original atomizer [9]:

$$\mathrm{Re} = \frac{w_i D_i}{\nu} \qquad (1)$$

where w_i is the velocity inside the inlet port, D_i is the hydraulic diameter of the inlet port and ν is the liquid kinematic viscosity.

Another important dimensionless number is the swirl number, S_0. This number is basically the ratio of the radius of the swirl chamber, the discharge orifice and cross-section of the inlet ports [3]. It has to be the same for the scaled model and the original atomizer. If the each part of the atomizer is scaled equally then the swirl number remains the same:

$$S_0 = \frac{\pi R r_0}{A_i} \qquad (2)$$

where R is radius of the swirl chamber, r_0 is radius of the exit orifice and A_i is total cross-section of inlet ports.

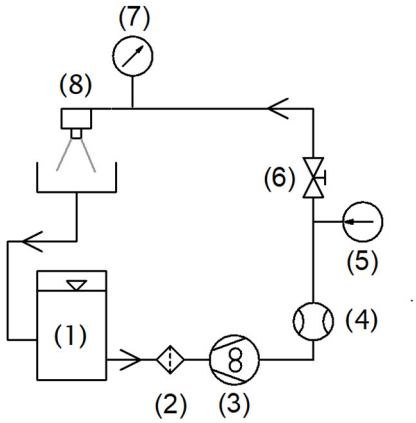

Fig. 1. Test bench

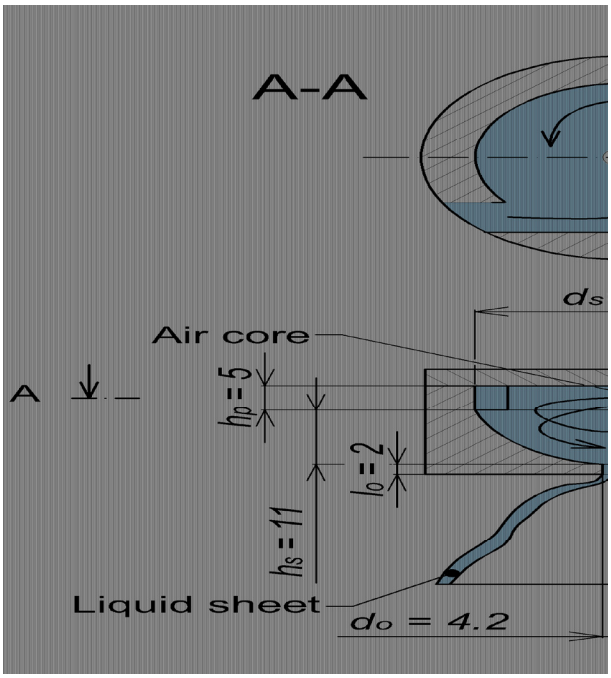

Fig. 2. Sketch of the transparent atomizer, main dimensions in millimetres. The original atomizer is ten times smaller.

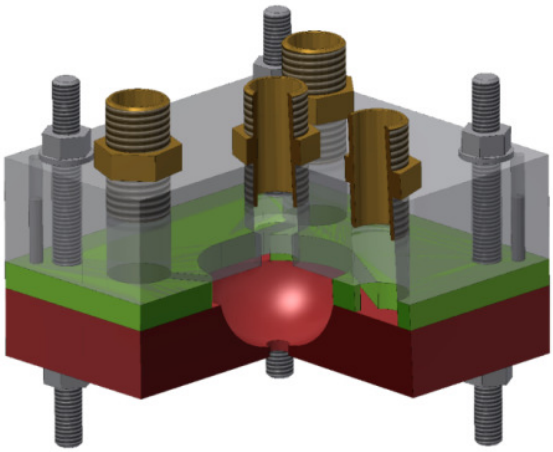

Fig. 3. Model of the scaled transparent modular atomizer

The Freude number shows the effect of gravity in comparison to the energy of the bulk flow [9]. This number must be high enough to minimalize the influence of gravity on the liquid flow:

$$Fr = \sqrt{\frac{u^2}{4r_0 g}} \quad (3)$$

Where u is axial velocity, r_0 is diameter of the orifice and g is gravitational acceleration.

Moreover, it is necessary to match the refractive index of the fluid with the one of the PMMA to allow optical measurement and visualizations inside the swirl chamber. The refractive index of original JET A-1 kerosene is 1.44 whereas the refractive index for PMMA is 1.49. Therefore, a number of different liquids and mixtures were tested to find the optimum liquid for the model

Table 1. Liquids properties at 20°C, refractive indices based on wavelength 660 nm

Liquid	ρ [kg/m^3]	n [-]	μ [mPa·s]	Damage after 10 days
Castor oil	960	1.479	986	None
Paraffin oil	850	1.48	21	None
Anise oil	981	1.557	2.37	Heavy
Turpentine	857	1.473	1.49	Slight
Tetraline	973	1.541	2.1	Partial
p-Cymene	860	1.49	0.876	Slight
Glycerine	1262	1.47	1480	None
Kerosene	785	1.44	1.6	None

The liquid corrosiveness to PMMA was tested using several liquids in undiluted form as well as in mixtures to achieve the exact refraction index of PMMA – see Table 1 and 2. Each mixture in table 2 has approximately the same refraction index as PMMA.

Table 2. Mixtures of liquids, refractive index matched with PMAA

Mixtures of liquids		Damage after 10 days
Anise oil +	Paraffin oil	Slight
	Turpentine	Partial
	Castor oil	Slight
	p-Cymene	Slight
	Glycerine	Not soluble
Tetraline +	Paraffin oil	Slight
	Turpentine	Slight
	Castor oil	Slight
	p-Cymene	Slight
	Glycerine	Not soluble

It can be concluded that the castor (ricinus) oil, paraffin oil and glycerol do not damage the PMAA at all. However, it would be difficult to use them due to their high viscosity and low refractive index. The liquids with a close refractive index to PMAA, e.g. p-Cymene and mixtures based on Anise oil or Tetraline always corroded the PMAA. For the sake of simplicity p-Cymene was chosen as a one-component operating liquid. Moreover, the refractive index of clean P-Cymene can be tuned also by temperature where an increase in temperature of about 1°C results in a decrease in the refractive index of approximately 0.0004 [10]. It is also colourless, has a low frothiness and damage to the PMMA was slight but acceptable.

After the first trial of p-Cymene as the working liquid, the atomizer was damaged, especially the parts with inlets and threads. The problem was linked to the internal stresses, which accelerates deterioration of the PMMA. This effect was not considered during the static tests.

Table 3. List of operating regimes

Original atomizer			
Re [–]	**Δp** [MPa]	**m_l** [kg/h]	**Fr** [–]
1560	**0.5**	5.41	137.4
2560	**1.5**	8.97	359.8

Transparent atomizer				
	Kerosene		**p-cymene**	
Re [–]	**m_l** [kg/h]	**Fr** [–]	**m_l** [kg/h]	**Fr** [–]
1560	54.1	6.9	29.0	3.4
2560	89.7	11.4	48.1	5.7

2.3 High speed imaging and LDA system

A Photron SA-Z high-speed camera was used to characterise the spatial and temporal behaviour of the air core. The atomizer was illuminated by a background light using an LED panel. The camera frame rate was 20,000 fps and image resolution was 1024 × 1024 px. The shutter speed was set to 20 µs.

The laser Doppler anemometer (LDA), a 2D FlowExplorer (Dantec Dynamics A/S), was employed for the point-wise measurement of the swirl and radial velocity in three cross-sections across the swirl chamber, see fig 5. The LDA used diode-pumped solid-state lasers and generated beams with 660 nm and 785 nm wave lengths. The beam was split into two pairs of parallel beams. Frequency of one beam from each pair was shifted by 80 MHz. A converging transmitting lens with 300 mm focal length was used to form an ellipsoidal probe volume with size approx. 0.1×0.1×0.7 mm at the beam crossing point. The LDA was configured in a backscatter mode.

The flow was seeded by silica particles e-spheres SL75 with mean diameter of 45 µm. The Stokes number, based on the swirl velocity and diameter of the swirl chamber, was less than 0.01 for each regime, which should ensure a sufficiently small flow traceability error.

During LDA measurements, several possible issues must be considered. The differences in refractive indices between the surrounding air, atomizer body and operating liquid cause displacements and distortion of the measuring volume due to different optical paths of each beam, see fig 4.

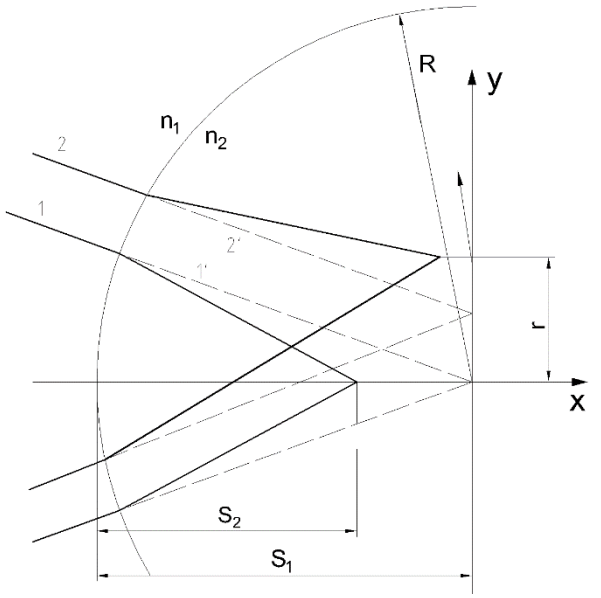

Fig. 4. Schematic drawing of beam path through the transparent model

Different issues arise in measurements of the swirl, radial and axial velocity component and must be taken in to account. Considering the matched refractive indices of liquid and atomizer body, the problem can be simplified to measurement in a planar window and thus only the position of the measurement volume must be corrected for as:

$$S_2 = \frac{n_2}{n_1} S_1 \qquad (4)$$

where n_1 and n_2 are refractive indexes of surrounding air and atomizer body, S_1 is the position of the measuring volume in the air, S_2 is the real position of the measuring volume inside the atomizer.

However, when the refractive index is not matched i.e. a difference greater than 0.01 then the circular geometry of the swirl chamber must be considered – see fig. 4. In the case of the swirl velocity component measurement, the optical plane is perpendicular to the atomizer axis, therefore, the properties of the measurement volume are dependent on the local position of the measurement point into flow [14]. Both, the position and velocity must be corrected.

Measurement of radial velocity component is even more complex and in the positions further from the atomizer centre, the optical aberration and measurement volume dislocation make the measurement almost impossible [14].

3 Results and discussion

The results are divided into two main parts: The air core shape based on the high-speed visualization and the velocity profiles based on the LDA measurements. Emphasis is placed on evaluation of refractive index effect in both cases.

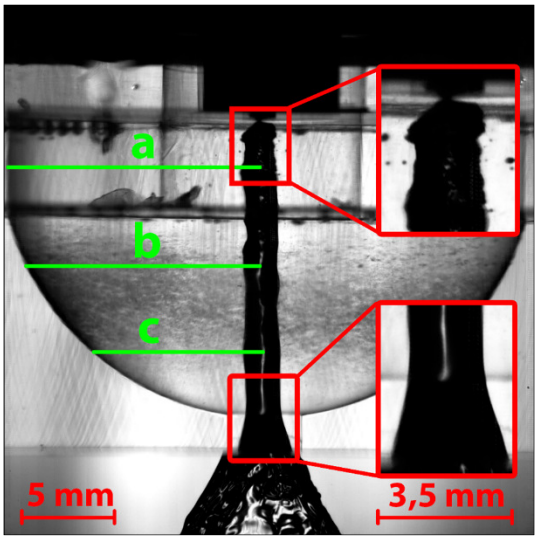

Fig. 5. Measurement positions

3.1 High speed visualization

In a comparative manner, the high-speed records with kerosene and p-cymene as the working liquid is shown in fig. 6. For the kerosene image there are darker region towards the edge of the swirl chamber. This is caused by light refraction at the swirl chamber wall. It is not evident in the atomizer centre due to the small relative curvature. This problem is overcome using the liquid with the same refractive index as the atomizer body as can be seen for the results from p-cymene.

A fully developed air core was found in all tested cases. It was cylindrically shaped with an extended diameter inside the exit orifice. Similarly shaped air cores were described by several authors [11, 12, 13]. The air core diameter (d_{ac}) inside the exit orifice was 3.09 ± 0.05 mm and it was equal for both liquids and inlet conditions. In the swirl chamber, the d_{ac} was 2.1 mm for both liquids at Re = 1560 and it decreased by 5 % with increasing Re.

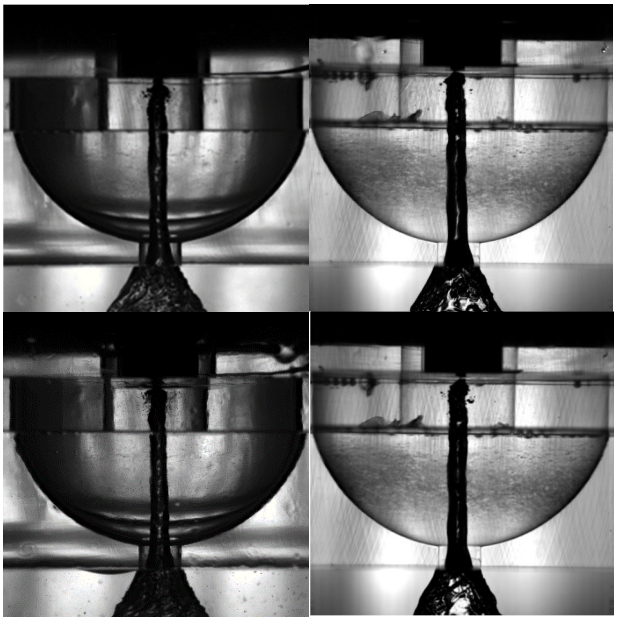

Fig. 6. High-speed image, from top: Re = 1560 and 2560, left: Kerosene, right: p-cymene

3.2 Velocity profiles

The swirl velocity profiles show a sharp maximum near the interface which is typical for Rankine vortex – see fig 7. This swirl velocity is almost independent of the axial distance from the top of the swirl chamber. For both liquids, the profiles had the same slope, however, in case of kerosene, the values are higher due to the higher flowrate used in order to keep the same Re. In positions close to the air-core, the raw velocity data were filtered since strong noise was generated by reflection from the air core surface.

The turbulence intensity (TI) was calculated as the ratio of the standard mean deviation to an average swirl velocity. Its dependence on radial distance is shown in fig. 8 for both liquids and pressure regimes in axial distance of 2.5 mm.

Increasing the inlet velocity (Re) in the inlet ports slightly decreased the turbulence intensity. Kerosene featured slightly higher turbulence level compared to p-cymene at the same Re. Strong increases in TI was found in positions near the wall and close to the air core.

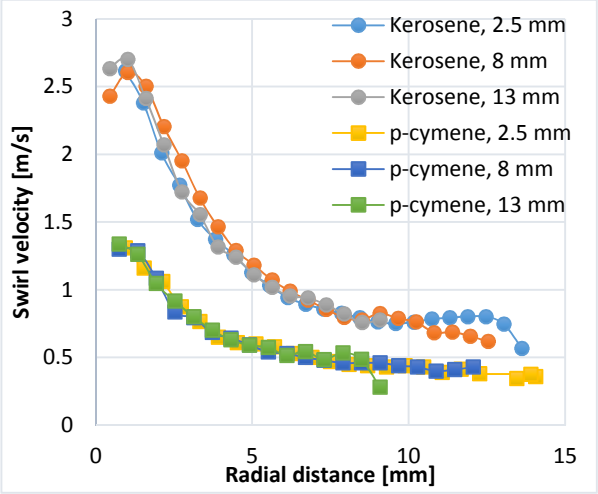

Fig. 7. Swirl velocity profiles for Re = 1560

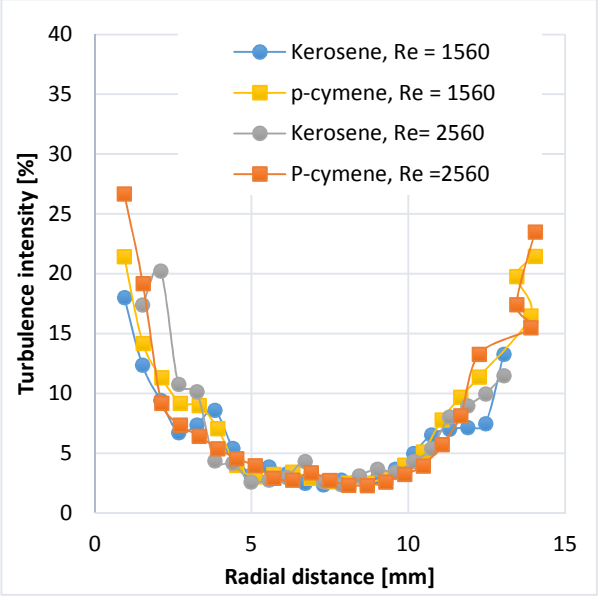

Fig. 8. Turbulence intensity, Z = 2.5 mm

However, the raw velocity data for TI were not filtered to remove effect of optical noise. This is evident in a sharp increase in TI for position very close to the atomizer centre. However, the impact for both liquid is very similar. The presence of large gradients in the swirl velocity may also result in a change of the velocity magnitude along the measuring volume itself which consequently leads to an apparent increase in the turbulence results. In the centre of the measurement plane across the swirl chamber, the TI was approximately 3 % which correspond to low turbulent flow. However, due to low Re in the inlet ports and the fact that the swirling flow tends to laminarise the flow itself [9], this near laminar nature of the flow is to be expected. Measured TI data may also be overestimated due to time-resolved flow fluctuations and general measurement inaccuracies.

To evaluate the effect of different liquid refractive indices, the LDA data-rate and validation rates were compared – see fig 9 and fig 10. In the case of swirl velocity (fig. 9), both liquids behaved similarly which was not expected. P-cymene had higher validation rate in positions closer to the atomizer centre. However, in positions close to the wall, both liquids had similar validation rates of over 70 %. The data-rate was found to be even less dependent on the liquid used. The difference is noticeable only close to the atomizer centre where the kerosene had higher data-rates compared to p-cymene. This behaviour may be caused by different concentrations of tracking particles which have a strong impact on data-rate. It can be concluded, that the difference in refractive index between kerosene and the atomizer body ($\Delta n = 0.05$) caused very small distortions of the LDA measuring volume in the case of the swirl velocity measurement.

The situation is different when the radial velocity is measured. The data-rate in the case of kerosene was about one order of magnitude lower compared to p-cymene. The difference is smaller in the positions near the atomizer centre as the relative curvature is also smaller.

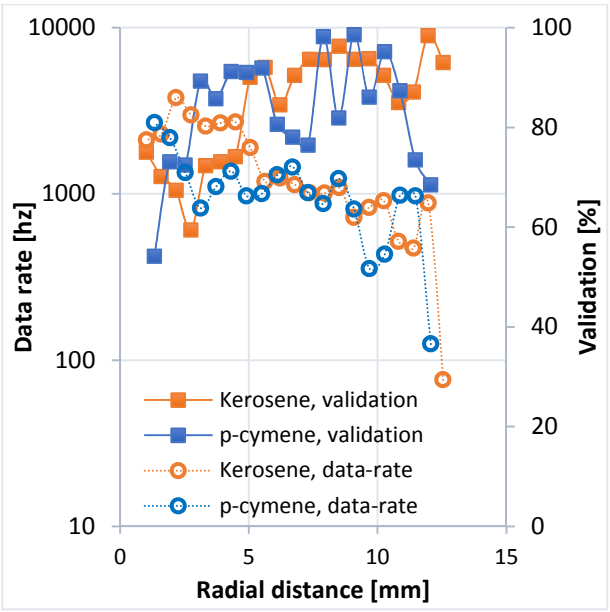

Fig. 9. Swirl velocity, data-rate and validation rate, Re = 1560, Z= 8 mm

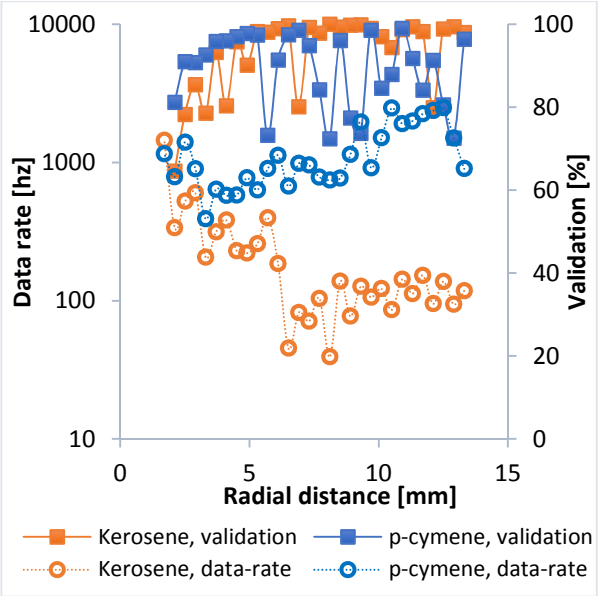

Fig. 10. Radial velocity, data-rate and validation rate, Re = 1560, Z = 8 mm

For positions higher then R/2 the laser beam deviations and optical aberrations corrupt the measurement volume and make measurements almost impossible. This is in agreement with [14]. The measured velocity data in positions with a greater diameter than R/2 are caused probably by noise, as the velocity magnitude is close to zero.

4 Conclusion

The internal liquid flow of a transparent pressure-swirl atomizer was investigated by high-speed imaging and LDA measurements using two liquids with different refractive indices.

The internal flow generates a stable, cylindrically shaped air core for both liquids under the pressure regimes studied. Swirl velocity profiles were found to be independent of axial location in the swirl chamber and had a sharp maximum near the air-core boundary, typical for a Rankine vortex.

Refractive index matching is necessary for the LDA measurement of radial and axial velocity components. However, there were only small difference in the case of swirl velocity measurements. Results from the high-speed imaging were independent of the liquid used.

This work has been supported by the project No. GA15-09040S funded by the Czech Science Foundation, the project LO1202 NETME CENTRE PLUS with the financial support from the Ministry of Education, Youth and Sports of the Czech Republic under the "National Sustainability Programme I" and project Reg. No. FSI-S-17-4444 funded by the Brno University of Technology.

References

1. M. Horvay, W. Leuckel, ALAFM, **2**, 18, (1985)
2. M. Horvay, W. Leuckel, *Experimental and Theoretical Investigation of Swirl Nozzles for Pressure-Jet Atomization.* (1986)
3. H.J.K De Keukelaere, MSc Dissertation, Dept. Mech. Eng., UMIST, (1995)
4. D. Cooper, J.J. Chinn, A.J. Yule, ILASS, **15**, (1999)
5. C.H. Liu, C. Vafidis, J.H. Whitelaw, EF, **10**, pp. 6, (1990)
6. B.E. Thomson, J. Senaldi, C. Vafidis, J.H. Whitelaw, H. McDonald, JSR, **29**, pp. 247-252, (1992)
7. Y.A. Hassan, E.E. Dominguez-Onziveros, NED, **238**, 6, (2008)
8. I. Muguercia, B. Cazanas, W. Li, M.A. Ebadian, SPIE, **2052**, 8 (1993)
9. J.J. Chinn, *The Numerics of the Swirl Atomizer*. Dept. Mech. Eng., UMIST, (2008)
10. M.P. Bardet, D.C. Fu, E.C. Sickel, A.N. Weichselbaum, ISALTFM, **17**, (2014)
11. M. Halder, S. Dash, S. Som, ETFS, **26(8)**, 8, (2002)
12. E.J. Lee, S.Y. Oh, H.Y. Kim, S.C. James, S.S. Yoon, ETFS, **34(8)**, 8, (2010)
13. G. Amini, IJMF, **79**, 10, (2016)
14. Z. Zhang, *LDA Application Methods: Laser Doppler Anemometry for Fluid Dynamics*, Springer, (2010)